Time-resolved measurement of plasma parameters in the far-field plume of a low-power Hall effect thruster

2012 Plasma Sources Sci. Technol. 21 055020

(http://iopscience.iop.org/0963-0252/21/5/055020)

Plasma Sources Sci. Technol. **21** (2012) 055020 (9pp) doi:10.1088/0963-0252/21/5/055020

Time-resolved measurement of plasma parameters in the far-field plume of a low-power Hall effect thruster

K Dannenmayer[1], P Kudrna[2], M Tichý[2] and S Mazouffre[1]

[1] Institut de Combustion, Aérothermique, Réactivité et Environnement, CNRS, Orléans, France
[2] Charles University, Faculty of Mathematics and Physics, Prague, Czech Republic

E-mail: kathe.dannenmayer@cnrs-orleans.fr

Received 14 March 2012, in final form 25 July 2012
Published 13 September 2012
Online at stacks.iop.org/PSST/21/055020

Abstract
Time-resolved measurements using electrostatic probes are performed in the far-field plume of a low-power permanent magnet Hall effect thruster. These measurements are necessary in order to account for the non-stationary behavior of the discharge. The plasma potential is measured by means of a cylindrical Langmuir and a sufficiently heated emissive probe, the electron temperature and density are measured with a cylindrical Langmuir probe. The thruster is maintained in a periodic quasi-harmonic oscillation regime by applying a sinusoidal modulation to a floating electrode in the vicinity of the cathode in order to guarantee repeatable conditions for all measurements. The modulation depth of the discharge current does not exceed approximately 10%. In order to achieve synchronism, the frequency of the modulation has to be close to the natural frequency of the observed phenomena. It is different depending on whether the discharge current or the plasma potential is selected as a reference. The measurements show that the fluctuations of the electron density follow the discharge current fluctuations. The time evolution of the plasma potential and the electron temperature is similar. The time-averaged properties of the discharge remain almost uninfluenced by the modulation. Measurements of the plasma potential with the two different probes are in good agreement. The observed phenomena are similar for Xe and Kr used as propellant gases.

(Some figures may appear in colour only in the online journal)

1. Introduction

Hall effect thrusters are advanced propulsion devices for space applications that use a cross-field discharge to ionize and accelerate a propellant gas [1, 2]. Such cross-field discharges are also used for different plasma applications such as magnetized plasma columns for fundamental studies of turbulence and instabilities [3], end-Hall ion sources for plasma processing and coating formation [4] or in the magnetic filter region of negative ion sources for neutral beam generation [5]. This work is focused on Hall effect thrusters.

The basic physics of a Hall thruster consists of a magnetic barrier in a low-pressure dc discharge maintained between an external cathode and an anode [1]. The anode, which also serves as gas injector, is located at the upstream end of a coaxial annular dielectric channel that confines the discharge. Xenon is used as a working gas for its specific properties in terms of atomic mass and low ionization energy. A set of solenoids or permanent magnets provides a radially directed magnetic field, the strength of which is maximum in the vicinity of the channel exit. The magnetic field is chosen strong enough to make the electron Larmor radius much smaller than the discharge chamber sizes, but weak enough not to affect ion trajectories. The electric potential drop is mostly concentrated in the final section of the channel owing to the high electron resistivity. The corresponding local axial electric field drives a high azimuthal drift—the Hall current—which is responsible for the efficient ionization of the supplied gas. It also accelerates ions out of the channel, which generates thrust. The ion beam is neutralized by a fraction of electrons emitted from the cathode.

The plasma in a Hall thruster is proved to be strongly non-stationary with many types of oscillations. Plasma and

discharge instabilities in the 1 kHz to 60 MHz frequency range have been observed during operation of Hall effect thrusters [6, 7]. The power spectrum of discharge and plasma instabilities in a Hall effect thruster is dominated by low-frequency oscillations in the kHz range, the so-called breathing mode [8, 9]. Two major interests exist for time-resolved measurements of the plasma parameters: first, anomalous transport is often attributed to turbulent plasma oscillations and low-frequency oscillations [10–13]. Second, time-averaged measurements of plasma parameters using Langmuir probes do not account for transient fluctuations of these parameters. However, strong plasma oscillations are known to distort probe measurements, hence rendering their accuracy questionable [14, 15]. The use of dc diagnostics may be responsible for differences between experimental data and numerical simulations in terms of anomalous transport, performances and erosion. Furthermore, accurate measurements of the plasma parameters are necessary for the validation of numerical plume models that are essential for the integration of plasma thrusters on the spacecraft.

Breathing mode oscillations are mainly investigated by observing the temporal behavior of the discharge current. Some experiments indicate that these oscillations can also be observed on the plasma parameters inside the discharge chamber or in the plume expansion near-field [9, 16, 17]. More recently Lobbia *et al* have shown that the transient fluctuations travel almost undamped throughout the entire far-field plume [18]. The aim of this study is thus to provide time-resolved measurements of the plasma potential V_p, the electron temperature T_e and the electron density n_e in the far-field plume of a low-power permanent magnet Hall effect thruster. The measurement technique is based on a phase-averaged approach. The main feature here is that the thruster discharge is maintained in a harmonic, low-frequency oscillation regime by applying a sinusoidal modulation on a floating electrode in the vicinity of the cathode. With the thruster operating in a synchronized regime, proper time-resolved measurements using Langmuir and emissive probes can be carried out, as the discharge current frequency content does not change in time. The plasma potential is measured with a cylindrical Langmuir probe and a heated emissive probe. The electron temperature and the electron density are measured with a cylindrical Langmuir probe.

2. Experimental set-up

2.1. Hall thruster

For the experiments the PPI Hall thruster was operated in a 1.8 m in length and 0.8 m in diameter vacuum chamber evacuated by a cryogenic pump. The PPI thruster is a 200 W Hall effect thruster able to deliver a thrust of about 10 m N at a discharge voltage of 250 V and a mass flow rate of 1.0 mg s^{-1} [19]. This low-power Hall thruster exhibits three interesting features [20, 21]. First, the magnetic field is provided by small SmCo magnets. The magnetic field strength can easily be varied by changing the number of magnets. Second, the gas is homogeneously injected through a porous ceramic instead of a classical metal hollow gas injector. A stainless steel ring placed at the end of the channel serves as anode. Third, a central copper heat drain and a radiator are used to reduce the thermal heat load. The PPI thruster used in this study has another interesting feature: the channel width can be varied while keeping the mean diameter and the channel length constant [22]. The experiments were performed with the largest channel, the so-called $3S_0$ configuration. The channel walls were made of alumina. A hollow heated cathode [23] was used with a cathode mass flow rate of 0.2 mg s^{-1}. Xenon and krypton were used as working gases for the thruster and the cathode. The thruster parameters, e.g. discharge current and cathode potential versus ground, were constantly recorded. The thruster was mounted onto two translation stages to allow a displacement in both the axial (x) and radial (y) direction.

2.2. Probes

A single cylindrical Langmuir probe was used to characterize the far-field plume of the PPI thruster. The Langmuir probe was made of a 0.38 mm in diameter tungsten wire. The non-collecting part of the wire was insulated from the plasma by a 100 mm long and 2 mm diameter alumina tube. The length of the collecting part was 5 mm. The probe axis was oriented parallel to the thruster axis. Since the Debye length was small compared with the probe radius we did not expect any irregularities in ion collection as described, e.g., in [24]. The voltage sweep and the resulting probe current measurement were performed using the ALP System^{TM} manufactured by Impedans. The measured electron energy distribution function was in its lower energetic part close to Maxwellian. Consequently, the parameters V_p, T_e and n_e were derived from the probe characteristics using the standard Langmuir probe theory assuming a Maxwellian electron distribution function [25].

The plasma potential was also measured using a floating emissive probe. The emitting part of the probe consisted of a 8 mm long loop of 150 μm in diameter thoriated tungsten wire. The ends of the wire were mechanically crimped to copper wires and inserted into two parallel holes of a 100 mm long and 4 mm diameter alumina tube. The filament was heated with a dc power supply up to the regime of electron emission. In the ideal case the floating potential of a sufficiently emitting probe is equal to the plasma potential. In this case the electron current is completely compensated by the emission current from the probe, therefore no net current flows through the probe and there is no sheath around the probe [26]. For the measurement of the plasma potential is assumed to be the floating potential of the probe heated with a current of 4.3 A.

Both probes were mounted next to each other in the far-field plume. The probes were oriented parallel to the thruster axis. An examination of the discharge current time evolution with and without the probes revealed that the probes do not influence the discharge behavior.

2.3. Time-resolved measurement technique

Several different methods have been developed for the acquisition of time-resolved data using Langmuir probes.

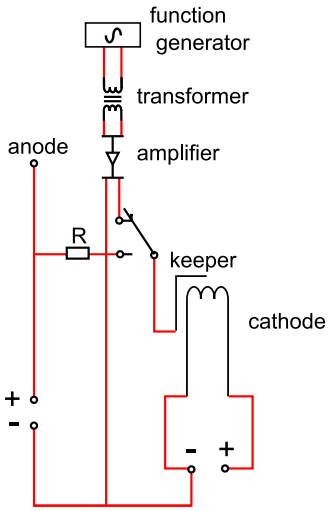

Figure 1. Schematic view of the electrical set-up of the keeper electrode modulation.

One possibility consists of rapidly sweeping the probe bias voltage with a frequency of up to 1 MHz [27]. The technical requirements for such a high-speed Langmuir probe system are very important. Furthermore, methods based on gating the probe bias or on fast sweeping the probe bias at a particular phase of the observed periodic plasma phenomenon are burdened with error arising from temporal response of the probe sheath [28]. Another possibility is to reconstruct the Langmuir probe I–V-characteristic from the time evolution of the probe current recorded for different probe bias voltages [17]. The idea of this method is based on the fact that the studied periodic plasma phenomenon changes much slower compared with the temporal response of the Langmuir probe under particular plasma conditions. The method consists of recording the temporal evolution of the probe current at a particular probe voltage. By repeating such measurements at many different probe voltages one obtains a 2D matrix of probe currents with time and voltage as independent variables. The time-dependent probe characteristics can easily be extracted from this matrix. This technique is mainly used for pulsed plasmas as the plasma behavior is stationary which warrants repeatable measurement conditions [30, 29]. In order to use this technique for a Hall thruster, the discharge needs to be maintained in a periodic quasi-harmonic oscillation regime. This has two main advantages: first, the harmonic signal can be used as trigger signal, hence no need for a fast power switch that perturbates the thruster behavior [31]. Second, the frequency content is fairly the same at any time, which warrants reproducible measurement conditions. Furthermore, time series can be added up without propagating noise and error.

To achieve a synchronized quasi-harmonic operating regime of the thruster, a sinusoidal potential with a tunable frequency is applied between a floating electrode, here the keeper electrode, and the negative pole of the cathode heating circuit. A schematic view of the electrical set-up is represented in figure 1. The modulation frequency cannot be chosen randomly, it has to be one of the resonance frequencies of the discharge. If an inappropriate frequency is chosen, no synchronization of the discharge parameters can be achieved, and hence no dominant frequency is visible on the power spectrum. In this case, proper time-resolved measurements are impossible, as reproducible measurement conditions cannot be guaranteed. In order to find the appropriate modulation frequency the time evolution of the discharge current, the cathode potential as well as the plasma potential measured with a heated emissive probe is monitored on an oscilloscope while adjusting the frequency. The modulation signal is provided by a function generator and amplified to achieve an amplitude of about 100 V. The modulation signal is applied by way of an isolation transformer to keep the keeper and the cathode insulated from ground. The square wave output of the function generator is used as a trigger signal for the ALP system in time-resolved mode. The current driven to the keeper is relatively low, and represents less than 10% of the discharge current.

The ALP system provides a time-resolved option. In this mode the probe current is recorded over one period of the modulation signal for a fixed bias voltage of the probe. This procedure is repeated for all the necessary voltage steps in order to reconstruct the current–voltage characteristics for every time step. In this work, the time resolution was set to 1 μs, the acquisition was averaged over 1000 records and the bias voltage was increased by steps of 0.2 V.

The time evolution of the potential of the heated emissive probe was recorded simultaneously to the discharge current oscillations. The power supply for the probe heating was powered via an isolation transformer in order to reduce the capacity against ground. If this capacity is very high, the oscillations of the probe potential cannot be observed as the capacity together with the inner resistance of probe forms a low-pass filter. The bandwith of our configuration was about 60 kHz.

3. Results

The thruster is operated at a discharge voltage of $U_\mathrm{d} = 200$ V and an anode mass flow rate of $\dot{m}_a = 1.0\,\mathrm{mg\,s^{-1}}$ (Xe or Kr) resulting in a mean discharge current of $I_\mathrm{d} = 0.93$ A for Xe and $I_\mathrm{d} = 0.84$ A for Kr. The background pressure in the vacuum chamber during thruster operation is about 3×10^{-5} mbar. The measurements are performed at three different axial positions (x = 100, 150 and 200 mm) and four respectively three different radial positions (y = 0, 18.5, 25 and 50 mm), where $x = 0$ mm corresponds to the thruster exit plane and $y = 0$ mm corresponds to the thruster axis.

3.1. Influence of keeper modulation

As has been mentioned before, in order to perform proper time-resolved measurements, the thruster discharge needs to be in a periodic quasi-harmonic regime. Figure 2 represents the time evolution of the discharge current I_d, the cathode-to-ground potential CRP and the plasma potential V_p as a function of the modulation frequency for the PPI thruster operating at 200 V and $1.0\,\mathrm{mg\,s^{-1}}$ (Xe). The corresponding power spectrum is shown in figure 3. The plasma potential is measured with a heated emissive probe. The time evolution

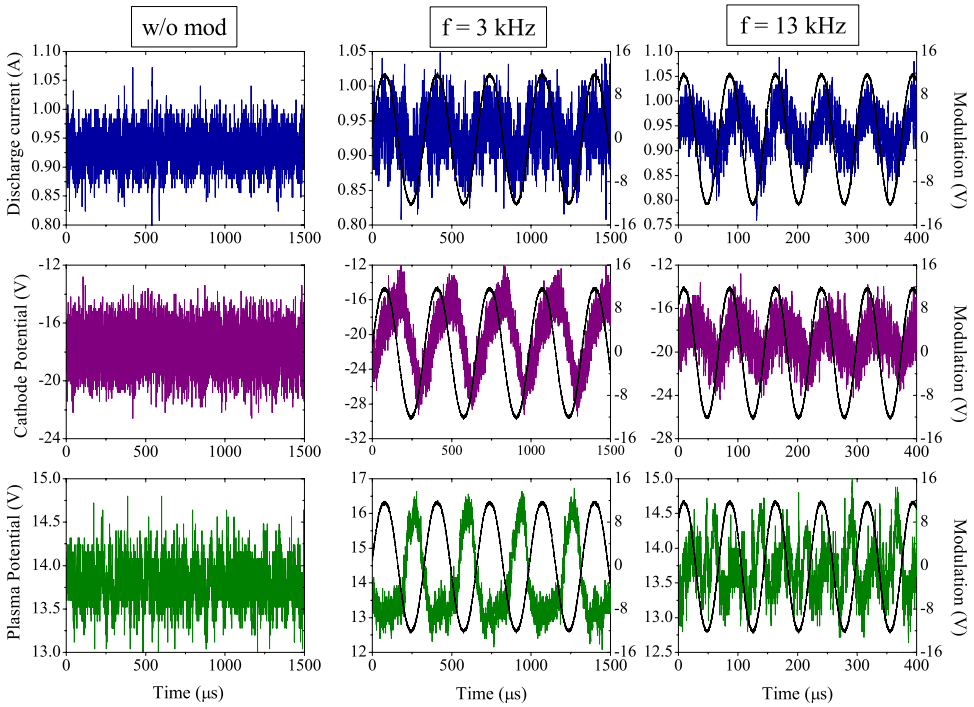

Figure 2. Influence of the keeper modulation on I_d, CRP and V_p for the PPI thruster operating at $U_d = 200\,V$, $\dot{m}_a = 1.0\,mg\,s^{-1}$ (Xe). The solid black line represents the modulation signal.

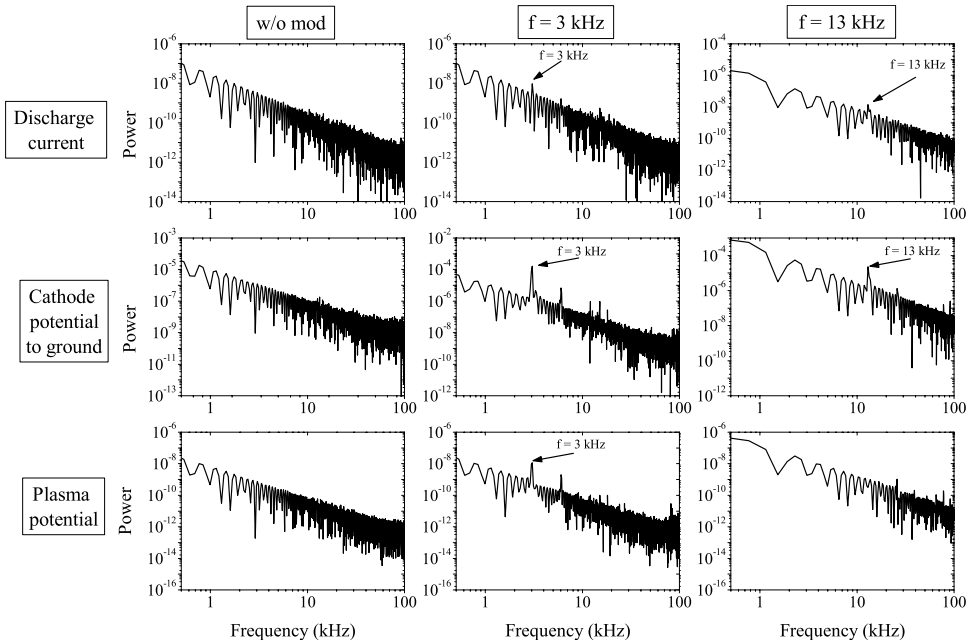

Figure 3. Power spectrum of the discharge current, the cathode potential and the plasma potential without modulation and for the two modulation frequencies.

of V_p is recorded at 100 mm downstream the thruster exit plane ($x = 100\,mm$) on the thruster axis ($y = 0\,mm$). As can be seen in figures 2 and 3, without a modulation signal, the discharge current is non-stationary and one cannot distinguish a dominant frequency in the discharge current time series, whereas for a modulation frequency of 13 kHz the discharge current is fairly well synchronized to the modulation waveform. The oscillation amplitude is not constant, but the oscillation frequency is constant. At a modulation frequency of 3 kHz, one can distinguish a slight synchronization of I_d to the modulation signal, but there are higher frequencies superimposed to the modulation frequency. In any case, the influence of the modulation on the mean discharge current is very weak ($\overline{I_d} = 0.93 \pm 0.004\,A$). The time evolution of the cathode potential to ground is represented in the second row of figure 2. The CRP is fairly well synchronized for both modulation frequencies. In contrast to the discharge current the mean value of the cathode potential is slightly different for

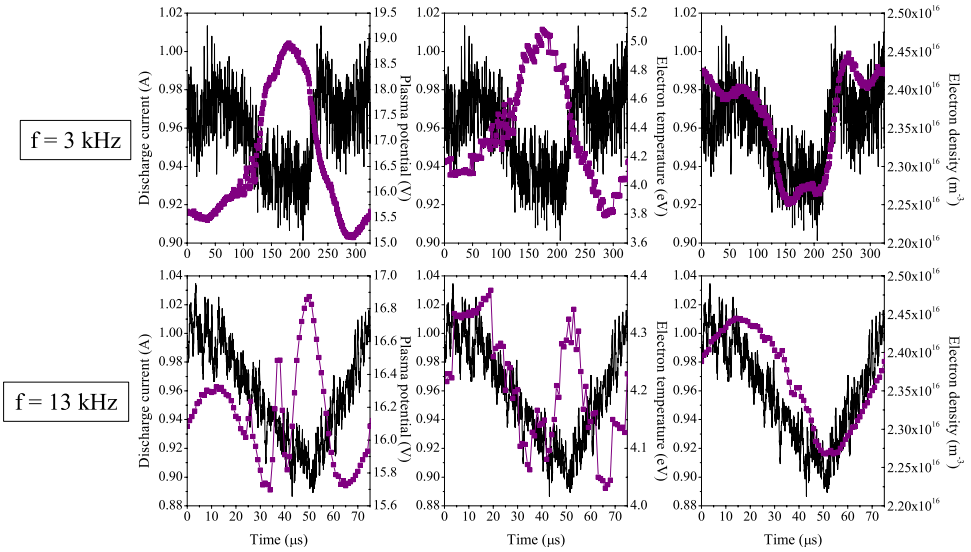

Figure 4. Time evolution of the plasma potential V_p, the electron temperature T_e and the electron density n_e measured by means of a Langmuir probe at $x = 100$ mm and $y = 0$ mm in the plasma plume of the PPI operating at $U_d = 200$ V, $\dot{m}_a$=1.0 mg s^{-1} (Xe). The discharge current I_d time series is shown as a solid line.

the three operating conditions ($\overline{CRP} = -18.79 \pm 1.25$ V). The third row of figure 2 shows the behavior for the plasma potential. Without modulation the plasma potential V_p is non-stationary and no dominant frequency can be distinguished. For a modulation frequency of 13 kHz, the time evolution of V_p is influenced by the modulation but no synchronization can be achieved and no dominant frequency is visible on the power spectrum. In contrast to the discharge current, the plasma potential can be stabilized if the modulation frequency is set to 3 kHz. Again the influence of the modulation on the mean value of the plasma potential is very weak ($\overline{V_p} = 13.85 \pm 0.18$ V).

3.2. Time evolution of plasma parameters

The time evolution of V_p, T_e and n_e in Xe for the two different modulation frequencies is displayed in figure 4 over one oscillation period. The first row represents the evolution over one period at 3 kHz, the second row the one for 13 kHz. The measurements are taken at 100 mm downstream of the thruster exit plane and on the thruster axis. The time evolution of the discharge current is also represented.

As can be seen in figure 4, the time evolution is different for V_p, T_e and n_e. There is also a difference between the results for the two different frequencies. The time evolution of the electron density at $f = 13$ kHz is almost sinusoidal, whereas the time evolution for $f = 3$ kHz is almost rectangular. Nevertheless, one can distinguish a high frequency oscillation superimposed to the basic rectangular n_e waveform. The frequency of this superimposed oscillation is about 13 kHz. However, for both frequencies changes are very weak, i.e. approximately 7% of the mean value. For both frequencies n_e follows almost exactly the time evolution of I_d. The phase delay between I_d and n_e is about 20 μs for the modulation at 13 kHz. At 3 kHz, there is no clear phase delay between I_d and n_e. For 3 kHz, the time evolution of V_p and T_e is almost the same and in phase opposition with the discharge current. At the modulation frequency of 13 kHz, the time evolution of V_p and T_e show some similarities, the location of the different peaks is the same but the peak amplitude is different. The time evolution of V_p and T_e is more complex than the one of I_d with a multi-peak structure. The fluctuations of V_p and T_e are significantly higher for 3 kHz than for 13 kHz, i.e. 23% against 7% for the plasma potential and 30% against 8% for the electron temperature.

Table 1. Mean values V_p, T_e and n_e on the thruster axis for three different distances downstream of the thruster axis.

Axial Position (mm)	3 kHz			13 kHz		
	V_p (V)	T_e (eV)	n_e (m^{-3})	V_p (V)	T_e (eV)	n_e (m^{-3})
100	16.5	4.4	2.4×10^{16}	16.2	4.2	2.4×10^{16}
150	11.4	2.2	1.2×10^{16}	11.3	2.2	1.2×10^{16}
200	9.1	1.7	7.7×10^{15}	8.9	1.7	7.7×10^{16}

Like the mean values of the thruster operating parameters (I_d and CRP), the mean values of V_p, T_e and n_e calculated from the time-resolved data over one period do not depend greatly on the two modulation frequencies, in contrast to their different time evolution, as can be seen in table 1.

3.3. Time and space evolution

The evolution in time (over one modulation period) and space (radial direction) of the plasma potential, the electron temperature and the electron density at 100 mm downstream of the thruster exit plane is exemplified in figure 5 for the two different modulation frequencies. The radial profile is interpolated from the four recorded radial positions. The plotted data are unsmoothed. The structure of the fluctuations that can be observed in the example trace in figure 4 can also be seen in the different contour plots represented in figure 5. One can see that V_p, T_e and n_e decrease with an increase in

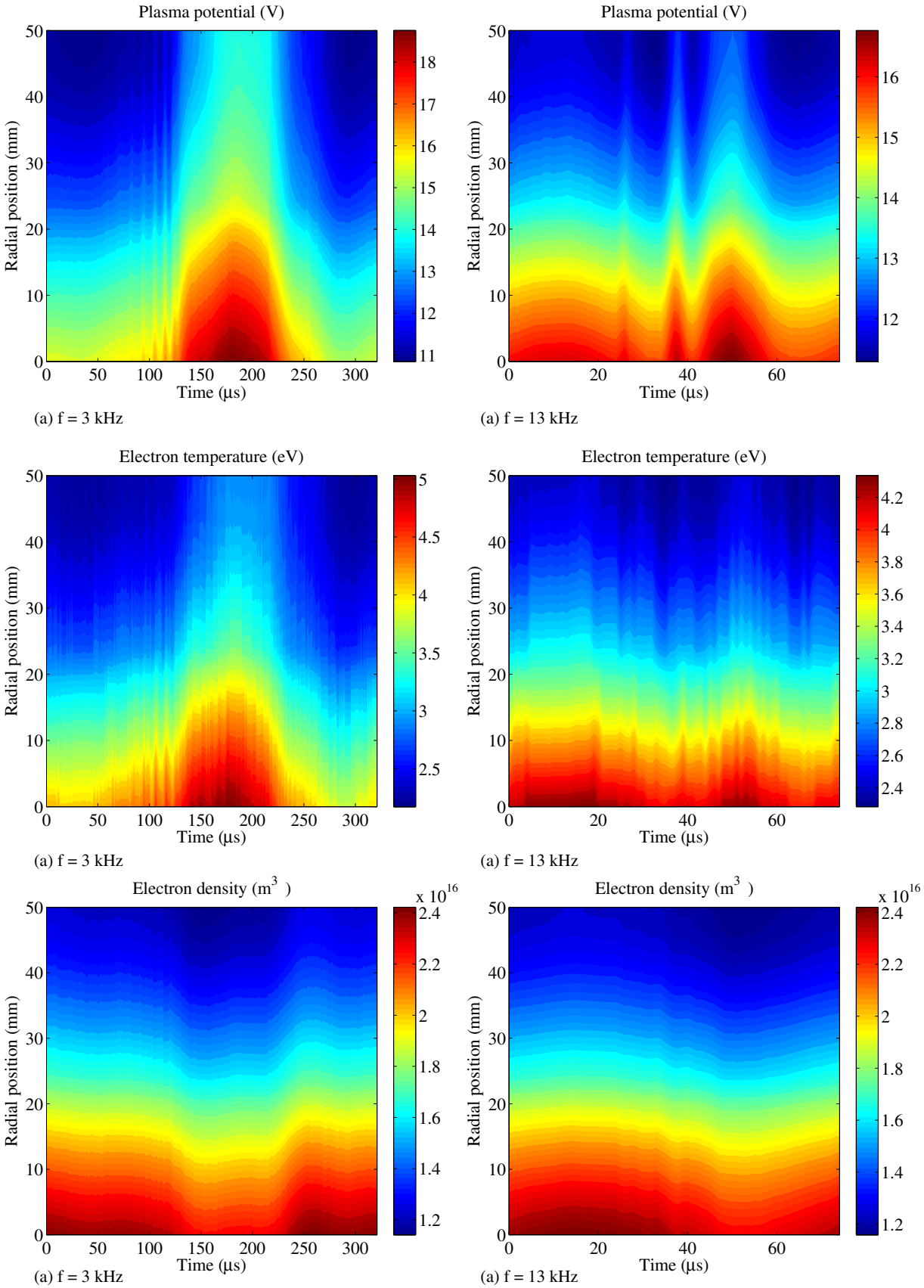

Figure 5. Evolution in time and space (radial direction) of V_p, T_e and n_e for the two different frequencies at 100 mm downstream of the thruster exit plane. The thruster is operated at $U_d = 200$ V, $\dot{m}_a = 1.0$ mg s^{-1} (Xe).

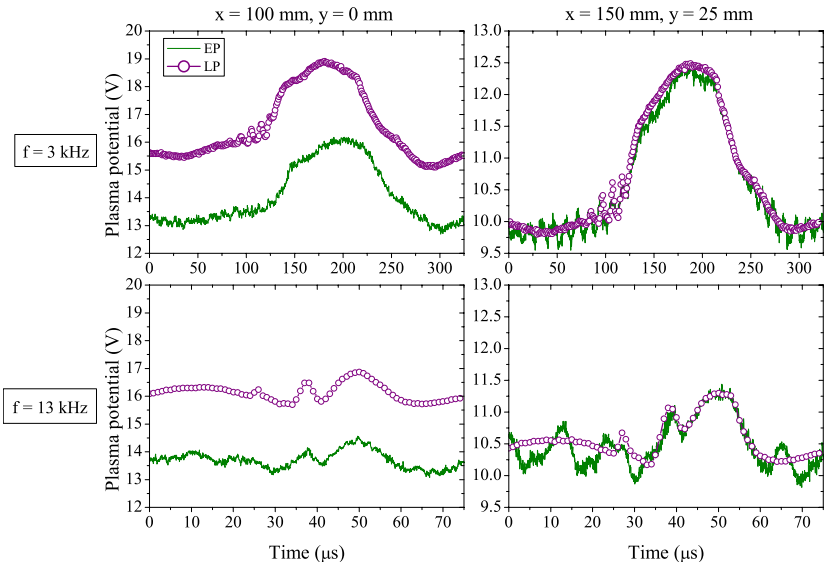

Figure 6. Comparison of the plasma potential measured with an emissive (green line) and a Langmuir (purple symbols) probe in the far-field plume of the PPI thruster operating at $U_d = 200\,V$, $\dot{m}_a = 1.0\,mg\,s^{-1}$ (Xe).

distance from the thruster axis (radial direction), as the plume is an expanding plasma jet.

3.4. Comparison between Langmuir and emissive probes

The time evolution of the plasma potential was also measured using an emissive probe. The plasma potential is assumed to be the floating potential of the emissive probe heated with a current of 4.3 A. The time evolution of the plasma potential is recorded simultaneously with the discharge current for the two different modulation frequencies. A comparison of V_p measured either with a Langmuir or an emissive probe is represented in figure 6 for the two modulation frequencies and at two different positions in the far-field plume. The time evolution of V_p over one period measured by the emissive probe is averaged over six periods.

The first column of figure 6 shows the time evolution of V_p on the thruster axis 100 mm downstream of the thruster exit plane (position 1). As can be seen V_p measured with the emissive probe is lower than V_p measured with the Langmuir probe. The second column shows the time evolution of V_p 25 mm off the thruster axis and 150 mm downstream of the thruster exit plane (position 2). The two time series of V_p coincide almost perfectly although the absolute values are different for position 1. It has already been shown before that the temperature of the electrons has an influence on the difference between the real plasma potential and the plasma potential measured by the emissive probe as the floating potential of the sufficiently heated probe [32, 33]. Due to space-charge effects, the accuracy of the plasma potential determined by the floating potential of an emissive probe is in the order of T_e/e [34, 35]. The accuracy is thus better at position 2, where the temperature of the plasma electrons is about 2 eV than at position 1, where T_e is about 4.4 eV.

The results for a modulation frequency of 3 kHz are shown in the first row of figure 6. As can be seen, the time evolution of V_p measured with both probes is identical. In contrast, for a modulation frequency of 13 kHz, the time evolution measured with the emissive probe is slightly different than the one measured with the Langmuir probe, as can be seen in the second row of figure 6. For 3 kHz, V_p is well synchronized and therefore an average over six periods is enough to obtain the global temporal behavior of V_p as measured by the Langmuir probe with an average of 1000 cycles. Since for a frequency of 13 kHz, the synchronization of V_p is worse, an average over six periods is not enough to obtain the global temporal behavior of V_p. However, as for the Langmuir probe, the mean values measured by the emissive probe are almost identical for the two modulation frequencies.

Despite the differences for the values of V_p obtained by means of emissive and Langmuir probe, the results are still in fairly good agreement. Both probes show the same time evolution of V_p. Even if the value of V_p may be slightly underestimated, emissive probes can be used to get a direct and instantaneous measurement of V_p. No voltage sweep or analysis of the current–voltage characteristic are needed as for a Langmuir probe.

3.5. Comparison between xenon and krypton

In order to evaluate the influence of the working gas on the plasma parameters, the PPI thruster was operated at 200 V with xenon and krypton. In both cases, an anode mass flow rate of $1.0\,mg\,s^{-1}$ was used. The modulation frequencies for the two gases are slightly different: in order to obtain a harmonic oscillation of I_d, the frequency is 13 kHz for Xe and 12 kHz for Kr, the plasma potential V_p can be maintained in a harmonic regime with a frequency of 3 kHz for Xe and 2 kHz with Kr. As explained in section 2.3, the appropriate modulation frequency is found by monitoring the time evolution of I_d, CRP and V_p while adjusting the frequency. The time evolution of V_p, T_e and n_e over one period of the oscillation for Xe and Kr is represented in figure 7. As the modulation frequencies are different, the time evolution is represented over one normalized

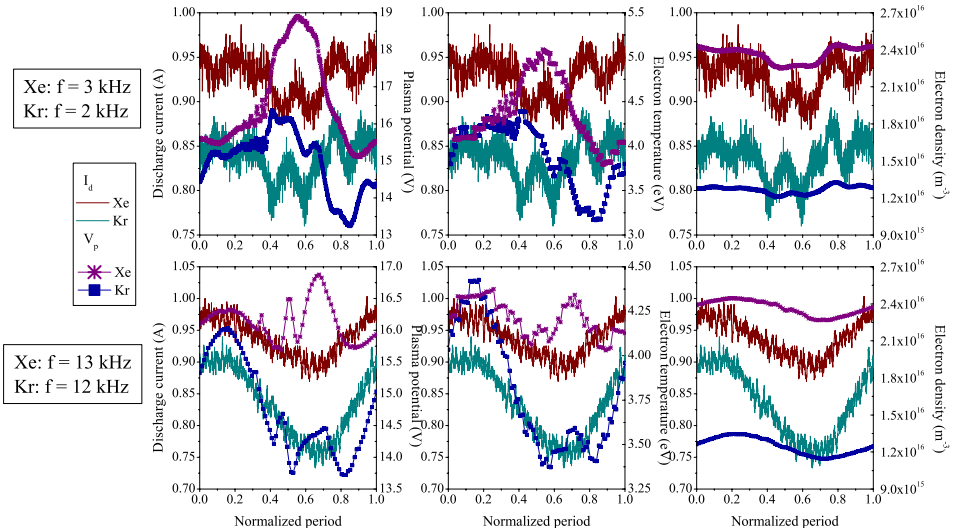

Figure 7. Comparison of the time evolution over one period of V_p, T_e and n_e for Xe and Kr for the two different frequencies at 100 mm downstream of the thruster exit plane on the thruster axis.

period. The time evolution of the discharge current is also represented. The measurements are performed on the thruster axis 100 mm downstream of the thruster exit plane.

As can be seen in figure 7, the time evolution of I_d and n_e is very similar for Xe and Kr. The time evolution of V_p and T_e is not exactly the same, but the global trend is similar. The values for all quantities are lower with Kr than with Xe. The modulation of the keeper electrode to maintain the thruster in a periodic quasi-harmonic oscillation regime works for both gases. The modulation frequencies are slightly different but the time evolution over one oscillation period is almost the same for the two gases meaning that the observed phenomena are independent of the propellant gas. The measurements of the plasma parameters were performed at four different radial positions for Xe ($y = 0$, 18.5, 25 and 50 mm) and three radial positions for Kr ($y = 0$, 18.5 and 25 mm). The mean values of the plasma parameters for the two different gases obtained from the time-resolved measurements are represented in figure 8. Note that also for Kr, the modulation has almost no influence on the mean values of I_d, V_p, T_e and n_e. As can be seen, the mean values for Kr are lower than the mean values for Xe, but the values decrease more slowly with an increase in distance from the thruster axis for Kr than for Xe.

4. Conclusion

In this paper, time-resolved measurements of the plasma potential, the electron temperature and the electron density in the far-field plume of a low-power Hall effect thruster are presented. A cylindrical Langmuir probe is used to measure V_p, T_e and n_e. The plasma potential is also measured with an emissive probe. In order to perform proper time-resolved measurements, the thruster is forced to a periodic quasi-harmonic regime by applying a sinusoidal modulation to a floating electrode in the vicinity of the cathode. The frequency of this modulation is adjusted to obtain a stable operating regime of the thruster synchronized to the modulation. The frequency required for thruster synchronization is different

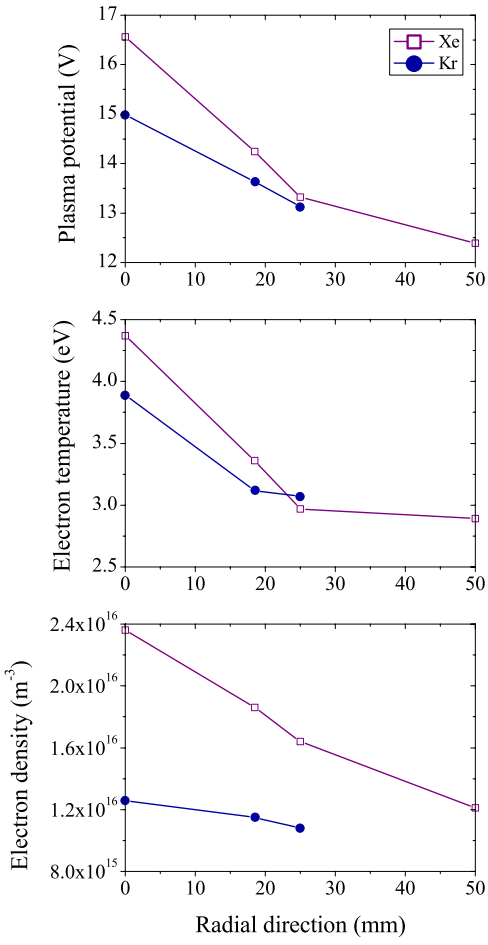

Figure 8. Comparison of the mean values of V_p, T_e and n_e measured with a Langmuir probe in the far-field plume of the PPI thruster operating with Xe (open squares) and Kr (circles) at $U_d = 200$ V, $\dot{m}_a = 1.0$ mg s^{-1}.

depending on whether the discharge current is observed or if one observes the plasma potential measured with a sufficiently heated emissive probe. The time evolution of V_p, T_e and n_e over one period is different for the two modulation frequencies.

However, the mean values remain almost uninfluenced by the modulations. It has been shown by a comparison of the plasma potential measured by means of a Langmuir and an emissive probe, that the latter can be used to get an instantaneous and direct measurement of V_p. Furthermore, it has been demonstrated that the presented measurement technique works for different gases (Xe and Kr). The required modulation frequencies depend on the propellant gas but the time evolution over one oscillation period is almost the same for both gases. It has been shown throughout the paper that the electron density fluctuations follow the discharge current oscillations. This can be explained by the fact that they both originate from the same phenomenon, namely the so-called breathing oscillation which is in fact an ionization instability [8]. Two different mechanisms can be put forward to explain the fluctuations of the electron temperature: first, collisions with heavy particles lead to a reduction in the electron temperature. In this case the fluctuation of n_e and T_e would be in phase opposition as the atom density is larger when the ionization degree is low. Second, the fluctuations of the electron temperature could also be due to the fluctuations of the electric field [31]. It has also been shown that the fluctuations of V_p and T_e are similar. This can be explained by the fact that a high electron temperature means that the electron speed is large. Hence, a higher plasma potential is necessary in order to maintain equilibrium.

Although the thruster is forced to a specific operating regime (periodic quasi-harmonic oscillation), neither the global thruster behavior nor the plasma parameters are significantly altered by the modulation. The presented method is thus a powerful technique for performing proper time-resolved measurements of the plasma parameters in a non-stationary cross-field discharge.

Acknowledgments

This work is carried out within the framework of the CNRS/CNES/SNECMA/Universités joint research program GdR 3161 entitled '*Propulsion par plasma dans l'espace*'. MT and PK acknowledge the financial support by CNRS contract 48792.

References

[1] Zhurin V V, Kaufmann H R and Robinson R S 1999 *Plasma Sources Sci. Technol.* **8** R1–2
[2] Kim V 1998 *J. Propul. Power* **14** 736
[3] Annaratone B M, Escarguel A, Lefevre T, Rebont C, Claire N and Doveil F 2011 *Phys. Plasmas* **18** 032108
[4] Oudini N, Hagelaar G J M, Boeuf J P and Garrigues L 2011 *J. Appl. Phys.* **109** 073310
[5] Kolev St, Lishev St, Shivarova A, Tarnev Kh and Wilhelm R 2007 *Plasma Phys. Control. Fusion* **49** 1349–69
[6] Choueri E Y 2001 *Phys. Plasmas* **8** 1411–26
[7] Morozov A I and Savelyev V V 2000 Fundamentals of stationary plasma thruster theory *Reviews of Plasma Physics* vol 21, ed B B Kadomtsev and V D Shafranov (New York: Consultant Bureau)
[8] Boeuf J P and Garrigues L 1998 *J. Appl. Phys.* **84** 3541–54
[9] Kurzyna J *et al* 2005 *Phys. Plasmas* **12** 123506
[10] Janes G S and Lowder R S 1966 *Phys. Fluids* **9** 1115
[11] Boniface *et al* 2006 *Appl. Phys. Lett.* **89** 161503
[12] Connor J W *et al* 2009 *Nucl. Fusion* **49** 047001
[13] Nedospasov A V 2009 *Phys. Plasmas* **16** 060501
[14] Matsumoto K and Sato M 1983 *J. Appl. Phys.* **54** 1781
[15] Oksuz L, Soberón F and Ellingboe A R 2006 *J. Appl. Phys.* **99** 013304
[16] Chesta E *et al* 2001 *IEEE Trans. Plasma Sci.* **29** 582–91
[17] Albarède L, Mazouffre S, Bouchoule A and Dudeck M 2006 *Phys. Plasmas* **13** 063505
[18] Lobbia R B and Gallimore A D 2008 *Proc. 44th Joint Propulsion Conf. (Hartford, CT)* AIAA 2008-4650
[19] Leufroy A, Gibert T and Bouchoule A 2009 *Proc. 31th Int. Electric Propulsion Conf. (Ann Arbor, MI)* IEPC 09-083
[20] Guyot M, Renaudin P, Cagan V and Boniface C 2007 *patent FR 07 05658*
[21] Guyot M *et al* 2008 *Proc. 5th Int. Spacecraft Propulsion Conf. (Heraklion, Greece)*
[22] Lejeune A, Dannenmayer K, Bourgeois G., Mazouffre S, Guyot M and Denise S 2011 *Proc. 32nd Int. Electric Propulsion Conf. (Wiesbaden, Germany)* IEPC 2011-019
[23] Albarède L, Lago V, Lasgoceix P, Dudeck M, Bugrova A I and Malik K 2003 *Proc. 28th Int. Electric Propulsion Conf. (Toulouse, France)* IEPC 03-333
[24] Hester S D and Sonin A A 1970 *Phys. Fluids* **13** 1265–74
[25] Chung P M, Talbot L and Touryan K J 1975 *Electric Probes in Stationary and Flowing Plasmas: Theory and Application* (New York: Springer)
[26] Ionita C *et al* 2011 *Contrib. Plasma Phys.* **51** 264–70
[27] Lobbia R B and Gallimore A D 2010 *Rev. Sci. Instrum.* **81** 073503
[28] Smy P R and Greig J R 1968 *J. Phys. D: Appl. Phys.* **1** 351–9
[29] Pajdarová A D, Vlček J, Kudláček P and Lukàš J 2009 *Plasma Sources Sci. Technol.* **18** 025008
[30] Dean A G, Smith D and Plumb I C 1972 *J. Phys. E: Sci. Instrum.* **5** 776-778
[31] Mazouffre S and Bourgeois G 2010 *Plasma Sources Sci. Technol.* **19** 065018
[32] Marek A, Jílek M, Picková I, Kudrna P, Tichý M, Schrittwieser R and Ionita C 2008 *Contrib. Plasma Phys.* **48** 491–6
[33] Dannenmayer K, Kudrna P, Tichý M and Mazouffre S 2011 *Plasma Sources Sci. Technol.* **20** 065012
[34] Ye M Y and Takamura S 2000 *Phys. Plasmas* **7** 3457–63
[35] Takamura S, Ohno N, Ye M Y and Kuwabara T 2004 *Contrib. Plasma Phys* **44** 126–37